

Liquid-Liquid Phase Coexistence in Gold Clusters: 2D or not 2D?

Pekka Koskinen,^{1,2} Hannu Häkkinen,³ Bernd Huber,² Bernd von Issendorff,² and Michael Moseler^{1,2}

¹*Fraunhofer-Institut für Werkstoffmechanik IWM, Wöhlerstr. 11, 79108 Freiburg, Germany*

²*Fakultät für Physik, Stefan-Meier Strasse 21, 79104 Freiburg, Germany*

³*Department of Physics, NanoScience Center, 40014 University of Jyväskylä, Finland*

PACS numbers:

It is well-known that first order phase transitions in small systems are broadened due to finite size effects. Instead of the concurrent coexistence of phases in bulk matter, a dynamical coexistence is observable over a finite, system-size-dependent range of a thermodynamical parameter, such as the temperature¹. A classic example is that of the liquid-solid phase coexistence in atomic clusters^{2–4}. Here we show by quantum molecular dynamics simulations that anionic gold clusters can exhibit a novel, free-standing planar (2D) liquid phase. This phase dynamically coexists with a normal three-dimensional (3D) liquid over a broad temperature range, thus representing a liquid-liquid coexistence (LLC). It is further shown that upon cooling with experimentally realizable cooling rates, the entropy-favored 3D-liquid clusters with $N > 12$ get supercooled and solidify into the “wrong” dimensionality. These results indicate that experimental validation of theoretically predicted gold cluster ground states might be more complicated than hitherto expected.⁵

Physical and chemical properties of gold in the nanoscale have attracted significant cross-disciplinary interest during recent years, motivated by some key observations of remarkable chemical and catalytic activity, electronic transport and optical properties. A large body of various structural investigations have led to the conclusion that gold in general prefers lower dimensional structures than other noble or late-transition metals due to strong relativistic bonding effects.^{6,7} This is manifested by its tendency to form relatively large planar^{5,7,8} or cage-like⁹ clusters. Another example is the formation of stable monatomic wires up to 7–8 atoms long as seen in mechanical break junctions,¹⁰ in separating tip-surface contacts,¹¹ or as a “nanobridge” in a free-standing thin gold film after intense electron irradiation.^{11,12}

Atomic clusters offer an ideal “laboratory” to study structure of matter as a function of size, and a considerable effort has been put forth to resolve preferred atomic geometries of anionic gold clusters (Au_N^- , $N \leq 20$) in the gas phase. Mobility measurements have previously detected a cross-over between 2D and 3D structures at $N = 12$.⁵ On the other hand, density functional theory (DFT) calculations employing the generalized gradient

approximation (GGA) predicted planar ground states for $N = 13$ and 14 ^{5,8} leading to the suggestion that GGA-DFT overestimates the stability of planar anionic clusters. This is a puzzling and unsatisfactory situation, especially given that GGA-DFT correctly describes the energetic sequence of smaller gold cluster isomers, as has been confirmed by photoelectron spectroscopy e.g. for $N=4, 8, 10$ and 12 .⁸

Motivated on one hand by this discrepancy between theory and experiment, and on the other hand by the fundamental question of the thermodynamic stability of low-dimensional nanostructures, we have investigated the dynamics of the liquid phase and the solidification transition of gold cluster anions from Au_{11}^- to Au_{14}^- using a recently established charge self-consistent density-functional based tight-binding (DFTB) model for gold¹³. Because our DFTB model is more than three orders of magnitude faster to solve than the full Kohn-Sham DFT model, while still retaining the essential electronic-structure effects, we were able to calculate thermodynamical properties and simulate the cluster cooling process within an experimentally realistic time scale. These simulations resulted in two unexpected and novel phenomena that we now discuss.

We first investigated the dynamics of hot liquid clusters via several microcanonical and canonical DFTB molecular dynamics (MD) runs at elevated temperatures up to 1100 K. Figure 1a shows the evolution of potential energy during a representative microcanonical MD run of Au_{14}^- with an average temperature of about 750 K. The potential energy can be observed to have a bimodal character (see inset to Fig. 1a) which is directly connected to abrupt changes in the dimensionality of the cluster (Fig. 1b). A careful analysis of the trajectory reveals that both the 2D and 3D phases are liquid, and since the bimodality is characteristic of coexistence¹⁴, we conclude that the clusters display a novel *liquid-liquid coexistence*. To the best of our knowledge, this is the first report of a free-standing *two-dimensional liquid* phase. This is not necessarily a typical behaviour of two-dimensional systems; corresponding simulations with small graphene clusters, for example, resulted in branched carbyne molecules instead of the establishment of a stable two-dimensional carbon liquid.

The liquid nature of the phases was confirmed using various, well established measures. First, inspecting the

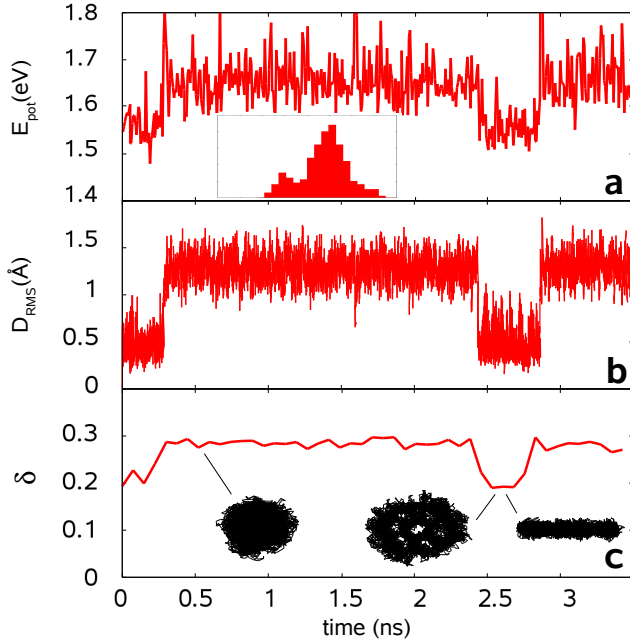


FIG. 1: **Dynamical coexistence of 2D and 3D liquid Au_{14}^- clusters.** Time-evolution of **a** the potential energy E_{pot} . Inset: histogram of potential energy short time averages (same energy scale as main panel). **b** planarity parameter D_{RMS} which is the root-mean-square deviation of the atoms from a plane defined by the cluster’s two largest radial dimensions ($D_{\text{RMS}} = 0$ strictly planar) **c** root-mean-square bond length fluctuation δ in a microcanonical DFTB molecular dynamics simulation of 3.5 ns corresponding to average temperature $T \sim 750$ K. Insets: trajectories of the atoms over 300 ps periods at high- and low-potential energy regimes.

case of Au_{14}^- more closely, figure 1c shows that the mean bond length fluctuation δ in the coexistence region remains above 20 %, a value identified with a liquid phase for even smaller clusters.¹⁵ Second, the diffusion constant $1 - 5 \cdot 10^{-5} \text{ cm}^2/\text{s}$ in the coexistence region is in a typical range of values for liquid, even though we find that it is typically 20 – 30 % lower in the 2D phase.¹⁶ This accounts for the fact that since atoms cannot escape from the plane, the motion of the atoms in 2D show up more correlated than in 3D, diminishing diffusion and bond length fluctuations. Third, the heat capacities of both planar and three-dimensional clusters increased from the almost exact Dulong-Petit value for low temperatures by more than 60 % upon heating to $T=750$ K - an increase characteristic for a hot liquid phase. Finally, a visual inspection of trajectories of the atoms over 300 ps periods at high- and low-potential energy regimes of the simulation confirms the existence of liquid-like 3D “drops” and 2D “disks” (insets of figure 1c).

The characteristics of the DFTB potential energy land-

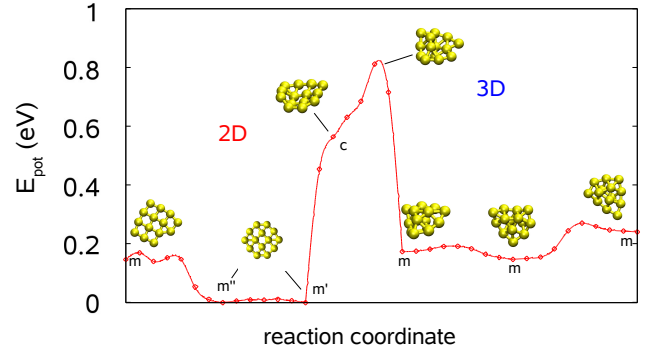


FIG. 2: **Characteristic barriers of Au_{14}^- .** A portion of the DFTB potential energy landscape at $T=0$, showing a few 2D and 3D local minima (marked by m), appearing also at high-temperature DFTB molecular dynamics runs. The very low 2D/2D barrier (m'/m'') represents a partial rotation of the 2D ground state, where the inner square rotates inside the 10-atom ring.

scape were investigated by calculating transition inter-conversion barriers for different stable isomers by the nudged elastic band method¹⁷. Figure 2 shows a portion of the DFTB potential energy landscape, showing a few 2D and 3D local minima (marked by m). The barriers within 2D and 3D regions are relatively low, which enables the separate 2D and 3D liquid phases. On the other hand, the phases are separated by a much higher 2D/3D barrier, which is a necessary condition for LLC. Note that the 2D/3D transitions are found to be preceded by a strongly excited 2D bending mode, such as the configuration before the 2D/3D transition state (marked by c). The DFTB barrier structure was confirmed by making similar nudged elastic band calculations using GGA-DFT^{18,19}. In order to have reasonable guesses for low transition pathways on the DFT Born-Oppenheimer surface, a 10 ps MD trajectory at 1250 K was simulated. Starting from the planar ground state, it was observed that also in GGA-DFT the planar structures are thermodynamically very stable. The heights of the chosen 2D/2D and 3D/3D barriers were significantly lower than the 2D/3D barriers, confirming the qualitative features of the DFTB energy landscape.

Next we turn our attention to the cooling processes that take place in the experiments. In a typical experimental source, noble metal clusters are grown in helium buffer gas by aggregation of metal atoms. Each aggregation event rises the internal temperature of clusters of sizes as considered here by about 1000 K; during aggregation and especially after the last atom attachment the clusters are cooled down again by collisions with the helium carrier gas. Rough estimates as well as previous

theoretical work²⁰ yield a typical cooling rate of about 0.1 eV/ns for a cluster with a kinetic temperature of around 700 K in a laser evaporation source (helium pressure about 100 mbar) and of about 0.001 eV/ns in a magnetron sputter gas aggregation source (helium pressure ≤ 1 mbar). These cooling rates imply time scales in the range of 0.1 to 10 μ s, which are accessible with our DFTB molecular dynamics.

The collisional cooling was simulated via extensive DFTB-MD simulations where a single trajectory consisted of sequential microcanonical parts; between two successive parts the kinetic energy of the cluster was reduced by ~ 0.013 eV through randomized virtual collisions. We performed in total 20 independent cooling runs, five per cluster size in the range of Au_{11}^- to Au_{14}^- . Figure 3a shows the time evolution of the planarity parameter D_{RMS} for representative runs in this size range. It can immediately be seen that the smallest clusters Au_{11}^- and Au_{12}^- rather continuously and smoothly anneal and solidify to the planar ground state whereas Au_{13}^- and Au_{14}^- solidify to higher energy 3D structures from the 3D liquid - 3D solid coexistence phase; note that both GGA-DFT and DFTB predict planar ground-state structures in this size range. The solidification dynamics is nicely reflected in the evolution of the root-mean-square bond length fluctuation (Fig. 3b); for Au_{14}^- the LLC ends at $E_{tot} \sim 2$ eV followed by a 3D-liquid-3D-solid coexistence for $E_{tot} < 1.1$ eV corresponding roughly to temperatures below 300 K (see Fig. 3c for the partial caloric curves $T(E_{tot})$ of both dimensionalities).

Why do the larger clusters get supercooled and solidify into the “wrong” 3D isomer space in the time scale of our simulation? Out of the aforementioned five cooling runs for each cluster size, all the runs resulted in the ground state isomer for Au_{11}^- and Au_{12}^- , whereas for Au_{13}^- only two and for Au_{14}^- only one simulation resulted in planar ground state isomers. We can suggest a combination of two factors that increases the tendency for supercooling to the wrong dimensionality. First, as figure 3d shows, in the LLC region with $E_{tot} > 2$ eV, the entropy of the 3D liquid phase is more than $2 \cdot k_B$ larger than the entropy of the 2D liquid phase. This results in longer dwelling times in the 3D phase, as displayed by figures 1b and 3a. Second, as discussed already in the context of figure 2, the phases with different dimensionalities are separated by high potential energy barriers. Upon cooling, this causes the 2D/3D barrier to become impenetrable already at a relatively high total energy where the equilibrium constant (the ratio [time in 2D]/[time in 3D]) is still small due to free energy differences. The larger entropy at higher temperatures thus favors supercooled 3D clusters.

After establishing the theoretical prediction that certain gold cluster anions can be supercooled to metastable structures at experimental cooling rates, we now return to the experimental situation. As discussed in the in-

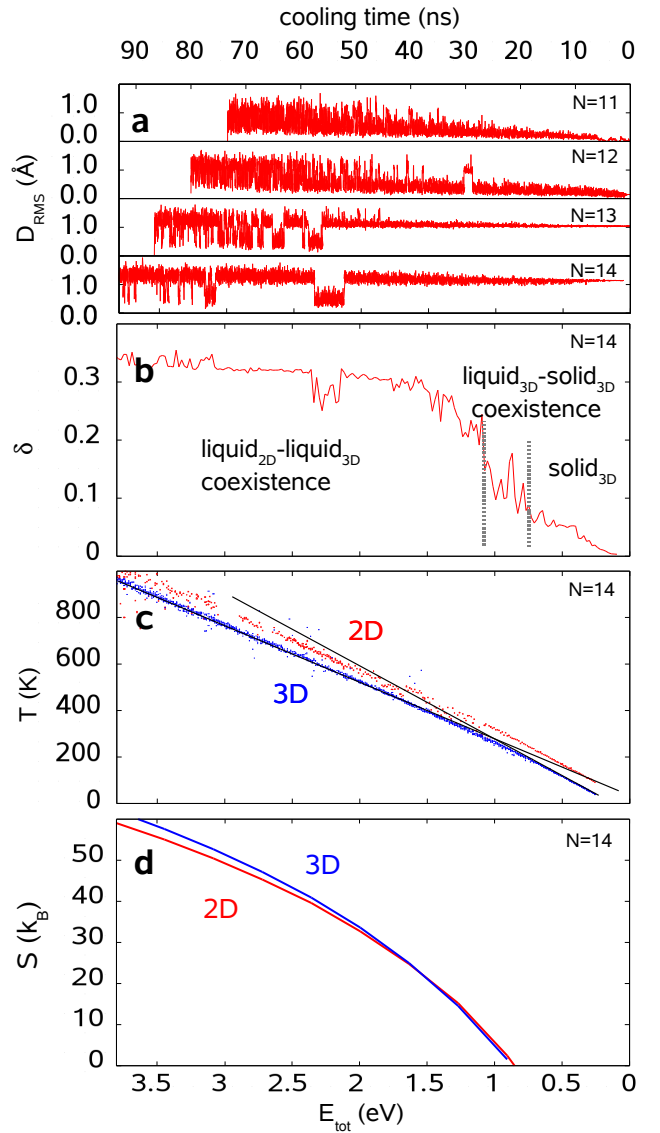


FIG. 3: Cooling simulations. **a**, Cooling simulations for $N = 11 \dots 14$ showing the planarity parameter $D_{RMS}(t)$. The scale on the x-axis above measures the cooling time (counted backwards) and total energy; it was started at $E = 2.99, 3.27, 3.54$, and 3.81 eV above the ground states of $N = 11, 12, 13$ and 14 , respectively, giving roughly $T = 1000$ K for initial temperature for each cluster size. **b**, Root-mean-square bond length fluctuation δ corresponding to the simulation for $N = 14$ in bottom panel of **a**. In the dynamical 2D liquid-3D liquid coexistence region the fluctuation is well above the conventional criterion $\delta > 0.1$ for liquids, valid also for clusters (for 2D δ jumps to smaller values due to smaller bond lengths and stiffer bonds in 2D). The cluster enters the 3D liquid-3D solid coexistence region near $E_{tot} = 1.1$ eV, where also δ is fluctuating, and becomes 3D solid around $E_{tot} = 0.77$ eV. **c**, The caloric curve for $N = 14$ was averaged over all five cooling simulations and separated into 2D and 3D phases making use of D_{RMS} . The planar clusters form the hot, low-potential energy phase. The 3D liquid phase has the heat capacity of $c_v = 4.05 k_B$ and the 3D solid phase $c_v = 3.06 k_B$ per atom (as obtained from the slope of the straight lines). A similar decrease of the heat capacity is obtained for the 2D solid-liquid transition. **d**, The partial entropies for 2D and 3D phases as a function of the potential energy (measured from the 2D ground state) calculated using the multiple histogram method^{21,22} and tight-binding simulations. The entropy curves have a cross-over around $E_{tot} = 1.5$ eV.

roduction, earlier collision cross section measurements with drift tubes⁵ suggested the 2D/3D transition size at $N = 12$ which lead to the speculation that GGA-DFT overestimates the 2D stability regime. Although this might be correct, it is not permissible to base this conclusion on a disagreement of experimentally determined isomers and theoretically predicted ground state structures, since with experimentally realizable cooling times it might just not be possible to reach a possibly existing 2D ground state. Thus, our results clearly underline the fact that even in small homogenous systems the possibility for supercooling (preferred formation of non-ground state structures) exists, which has to be taken into account when comparing experimental and theoretical results.

PK, BH, BvI and MM are grateful for the support of the Deutsche Forschungsgemeinschaft. PK acknowledges the Academy of Finland (AF) for a post-doctoral grant. HH and MM acknowledge a DAAD-AF bilateral travel grant. The DFT calculations were done at the John von Neumann Institute for Computing in Jülich.

-
1. D. J. Wales and R. S. Berry, Phys. Rev. Lett. **73**, 2875 (1994).
 2. R. S. Berry, J. Jellinek, and G. Natanson, Phys. Rev. A **30**, 919 (1984).
 3. M. Schmidt, R. Kusche, B. v. Issendorff, and H. Haberland, Nature **393**, 238 (1998).
 4. P. Labastie and R. L. Whetten, Phys. Rev. Lett. **65**, 1567 (1989).
 5. F. Furche, R. Ahlrichs, P. Weis, C. Jacob, S. Gilb, T. Bierweiler, and M. M. Kappes, J. Chem. Phys. **117**, 6982 (2002).
 6. P. Pyykkö, Chem. Rev. **88**, 563 (1988).
 7. H. Häkkinen, M. Moseler, and U. Landman, Phys. Rev. Lett. **89**, 033401 (2002).
 8. H. Häkkinen, B. Yoon, U. Landman, X. Li, H.-J. Zhai, and L.-S. Wang, J. Phys. Chem. A **107**, 6168 (2003).
 9. M. P. Johansson, D. Sundholm, and J. Vaara, Angewandte Chemie **43**, 2678 (2004).
 10. A. I. Yanson, G. Rubio-Bollinger, H. E. van den Brom, N. Agrait, and J. M. van Ruitenbeek, Nature **395**, 783 (1998).
 11. H. Ohnishi, Y. Kondo, and K. Takayanagi, Nature **395**, 780 (1998).
 12. V. Rodrigues and D. Ugarte, Phys. Rev. B **63**, 073405 (2001).
 13. P. Koskinen, H. Häkkinen, G. Seifert, S. Sanna, T. Frauenheim, and M. Moseler, New Journal of Physics **8**, 9 (2006).
 14. J. Jellinek, T. L. Beck, and R. S. Berry, J. Chem. Phys. **84**, 2783 (1985).
 15. H. L. Davis, J. Jellinek, and R. S. Berry, J. Chem. Phys. **86**, 6456 (1987).
 16. M. W. Mahoney and W. L. Jorgensen, The Journal of Chemical Physics **114**, 363 (2001).
 17. G. Henkelman and H. Jonsson, J. Chem. Phys. **113**, 9978 (2000).
 18. J. P. Perdew, K. Burke, and M. Ernzerhof, Phys. Rev. Lett. **77**, 3865 (1996).
 19. R. N. Barnett and U. Landman, Phys. Rev. B **48**, 2081 (1993).
 20. J. Westergren, H. Grönbeck, and A. Rosén, J. Chem. Phys. **109**, 9648 (1998).
 21. R. Poteau, F. Spiegelmann, and P. Labastie, Z. Phys. D **30**, 57 (1994).
 22. M. Moseler and J. Nordiek, Phys. Rev. B **60**, 11734 (1999).